Optimization Techniques for the Power Beaming Analysis of Microwave Transmissions from a Space-Based Solar Power Satellite

W. Feldman,[1] W. Gu,[1] A. Limon,[2] M. Kandes,[3,4,5] W. Kang,[6] and M. Rezaei[7]

[1] *Department of Mathematics, Harvey Mudd College, Claremont, California 91711, USA*
[2] *A&A Consulting, Temecula, California 92592, USA*
[3] *Computational Science Research Center, San Diego State University, San Diego, California 92182, USA*
[4] *Department of Physics, San Diego State University, San Diego, California 92182, USA*
[5] *School of Mathematical Sciences, Claremont Graduate University, Claremont, California 91711, USA*
[6] *Department of Applied Mathematics, Naval Postgraduate School, Monterey, California 93943, USA*
[7] *Department of Mathematical Sciences, Clemson University, Clemson, South Carolina 29634, USA*

Abstract

In the 21st century, the development of technologies to produce carbon free power sources remains paramount. In this paper, we study an optimal power transmission strategy from a space-based satellite generation station to Earth using scalar diffraction theory. The resulting model is then solved via a spectral method that guarantees a compactly supposed profile from the transmitting antenna. Finally, the problem is then solved via a more general pseudo-spectral method using control theory.

Introduction

Perhaps the single most important technological challenge currently facing humanity at the beginning of the 21st century is the problem of developing, producing, and storing sufficiently large scale supplies of carbon-free and/or carbon-neutral energy that will be able to meet future global energy demand in a sustainable way. By the year 2050, it is projected that worldwide energy consumption will require upwards of 28 terawatts (TW) of primary power [1, 2]. Although this requirement is more than double current worldwide energy consumption at 13 TW [1, 2], the easily accessible, ample supplies of non-renewable, carbon-intensive fossil fuel energy resources currently in use such as coal, oil, and natural gas will be more than adequate to make up this difference. However, in order to stabilize the increasing concentration of carbon dioxide in the Earth's atmosphere resulting from the emissions associated with the extensive use of fossil fuel energy resources and to mitigate the potential hazardous effects due to global climate change, it is estimated that more than 10 TW of this primary power will need to be delivered from carbon-free and/or carbon-neutral energy supplies [1, 2].

The largest, and potentially most scalable, resource of carbon-free energy available for global consumption is solar energy. The Earth receives approximately 174 petawatts (PW) of incoming solar radiation from the Sun at the upper atmosphere [3]. This amount of energy is more than 10,000 times the 10 TW carbon-free/carbon-neutral supply constraint that may be required to meet future global energy demands by 2050. Unfortunately, while solar energy is abundant enough to reduce the world's reliance on non-renewable, carbon-intensive energy resources and capable of meeting future global energy demands without significant environmental impact, the captial costs associated with solar energy technology are currently prohibitive [1, 2]. This is further complicated by geographic constraits that restrict its use to locations with cost-effective amounts of incident solar radiation. Even in such favorable locations, attenuation and interruption of solar radiation due to poor weather conditions and the day-night cycle leads to the requirement of an efficient and effective energy storage system to provide a dependable, baseload power supply from the solar energy conversion process. Moreover, any such system must account for losses associated with power distribution, e.g. from transmission line losses.

First proposed in 1968 by Peter E. Glaser [4], the space-based solar power satellite (SPS) concept attempts to overcome many of the limitations associated with the production, storage, and distribution of solar energy from traditional, terrestrial-based solar power systems. In the SPS system, a large solar photovoltaic array (PVA) is placed in geostationary Earth orbit (GEO) to convert solar energy directly into electricity. The electricity generated by the PVA of the SPS is then converted into microwaves by a microwave generator that forms part of a planar, phased-array antenna. This phased-array antenna then transmits the collected and converted solar energy back to the Earth in the form of a low power density microwave beam, which can be directed to one or more receiving antennas located on the Earth. At the receiving antennas, the microwave energy is reconverted into electricity and then distributed to users via transmission lines. The details of the SPS system are described thoroughly in [5] and [6].

There are several key advantages the SPS system has over traditional, terrestrial-based solar power systems. First, the PVA of the SPS in GEO is on average expose to between four and eleven times the average amount of incident solar radiation available at the surface of the Earth, which allows it to generate more power per unit area than any terrestrial-based system [5]. Secondly, and perhaps most importantly, because of its location in GEO, the PVA of the SPS avoids the major problem inherent to terrestrial-based solar power systems, namely, intermittency. In GEO, the incident solar radiation is available nearly continuously for 24 hours a day during most of the year [5]. This allows the SPS system to act as a natural baseload power supply, eliminating the need for complex energy storage systems required by terrestrial-based solar power systems built to operate in a baseload capacity. And lastly, because of the relative safety and low environmental impact associated with the transmission of microwaves through the atmosphere, the receiving antennas on the Earth in the SPS system can be situated near major power users to substantially reduce the overall cost of power transmission [7].

In this report, we focus on the power beaming problem in the SPS system. Specifically, we are interested in maximizing the power transmission efficiency in the microwave beam from the phased-array antenna of the SPS to a single receiving antenna located on the surface of the Earth. However, as a set of secondary constraints, in order to efficiently utilize the total collecting area of the receiving antenna on the ground, we must also consider distributing the intensity of the microwave beam as uniformly as possible across the area of the receiving antenna, while simultanelously minimizing the peak intensity of the sidelobes of beam that may fall outside this area, where the intensity of the beam will likely be more tightly controlled by government regulation for saftey purposes. In simplifying the geometry of this problem to make use of scalar diffraction theory, we assume that both the transmitting phased-array antenna of the SPS and the receiving antenna on the ground are planar and circularly-symmetric, with the additional simplification that both antennas are parallel and coaxially aligned with one another along the transmission axis of the microwave beam. This geometry is illustrated in Figure 1. To study the power beaming problem in this geometry, we employ both a spectral and pseudo-spectral optimization technique to solve this globally constrained optimization problem.

The report begins with a brief discussion on the underlying physical assumptions in standard scalar diffraction theory, which is used here to describe the propagation of electromagnetic radiation from the transmitting phased-array antenna of the SPS to the receiving antenna on the ground. In this discussion, we derive the Fraunhoffer approximation to the Huygens-Fresnel principle for a planar, circularly-symmetric phased-array antenna when the amplitude and phase of the transmitted wavefront is also circularly-symmetric. This approximation forms the fundamental basis of the objective functions used in the power beaming optimization problem considered later. We then outline the spectral and pseudo-spectral optimization techniques considered in this report. We conclude the report with some final remarks on the strengths and weaknesses of the optimization techniques considered in this work as they apply to the power beaming problem. We also discuss how they may be generalized when attempting to solve the more general power beaming problem with a less restrictive geometry.

Background

Electromagnetic radiation transmitted by a planar phased-array antenna can be well-described using scalar diffraction theory. Scalar diffraction theory assumes that the electromagnetic radiation transmitted by the phased-array antenna propagates within a dielectric medium that is linear, isotropic, homogeneous, nondispersive, and nonmagnetic. Under such conditions, all components of the electromagnetic field behave identically and their time-dependent behavior is fully described by the scalar wave equation [8]

$$\nabla^2 u(\mathbf{r},t) - \frac{n^2}{c^2}\frac{\partial^2 u(\mathbf{r},t)}{\partial t^2} = 0, \tag{1}$$

where $u(\mathbf{r},t)$ represents any of the scalar field components of the electromagnetic field. Here, the constants n and c are the refractive index of the medium in which the electromagnetic radiation is propagating and the speed of light in vacuum, respectively.

When the electromagnetic radiation transmitted by the phased-array antenna is monochromatic, any scalar field, $u(\mathbf{r},t)$, satisfying the scalar wave equation may be written explicitly as [8]

$$u(\mathbf{r},t) = \mathrm{Re}\left[U(\mathbf{r})e^{-i\omega t}\right], \tag{2}$$

where the time-independent complex function

$$U(\mathbf{r}) = A(\mathbf{r})e^{-i\phi(\mathbf{r})} \tag{3}$$

is defined in terms of the amplitude, $A(\mathbf{r})$, and phase, $\phi(\mathbf{r})$, of the electromagnetic wave at the position $\mathbf{r}$, while ω is the angular frequency of the electromagnetic wave. Since the time-dependence of the components of the electromagnetic field are known *a priori* when the radiation from the antenna is monochromatic, it follows from Equations (1) and (2) that the complex function $U(\mathbf{r})$ must obey the time-independent equation [8]

$$\left(\nabla^2 + k^2\right) U(\mathbf{r}) = 0. \tag{4}$$

The constant k is the wavenumber associated with the electromagnetic wave, which is related to the frequency and wavelength of the wave, f and λ, respectively, by the relation

$$k = 2\pi f\frac{n}{c} = \frac{2\pi}{\lambda}. \tag{5}$$

Note that Equation (4) is simply the well-known Helmholtz equation.

When the planar phased-array antenna is large compared to the wavelength of the electromagnetic radiation being transmitted and the electromagnetic field is not considered near the antenna, but is observed in a plane some distance away from the antenna, the general solution of the Helmholtz equation that relates the electromagnetic field in the plane of the antenna and the plane of observation is given by the well-known Huygens-Fresnel principle. In Cartesian coordinates, the Huygens-Fresnel principle is given by [8]

$$U(x,y) = \frac{z}{i\lambda}\int_{-\infty}^{\infty}\int_{-\infty}^{\infty} U(\xi,\eta)\ \frac{e^{ikd}}{d^2}\ d\xi\ d\eta, \tag{6}$$

where $U(\xi,\eta)$ and $U(x,y)$ represent the complex scalar components of the electromagnetic field distribution in the plane of the antenna and the observation plane, respectively. Here, we may consider the observation plane to be the plane in which the receiving antenna is located. The distance

$$d = \sqrt{z^2 + (x-\xi)^2 + (y-\eta)^2} \tag{7}$$

is the distance between any point located in the plane of the antenna and any other point located in observation plane, while z is the distance between the two planes. This diffraction geometry assumed by the form of the Huygens-Fresenl principle given in Equation (6) is illustrated in Figure 1. Although Figure 1

indicates the circular symmetry of the transmitting phased-array antenna assumed in this work (shown here as an oval in the ξ-η-plane), note that Equation (6) holds for any arbitrary shaped transmitting antenna provided the assumptions of scalar diffraction theory hold. Of course, by definition, the complex scalar component of the transmitted electromagnetic field, $U(\xi, \eta)$, is only non-zero on the closed surface of the tranmitting antenna, where the amplitude and phase of the electromagnetic radiation in the plane of the antenna are non-zero. Also shown in Figure 1 is the receiving antenna (which is depicted here as an oval in the x-y-plane) in the observation plane at a fixed distance of $z = h$ from the plane of the transmitting antenna. However, for generality, we consider the approximations to the Huygens-Frensel principle in the discussion below for all distances z. Finally, in Figure 1, a and b are the radii of the circular transmitting and receiving antennas, respectively.

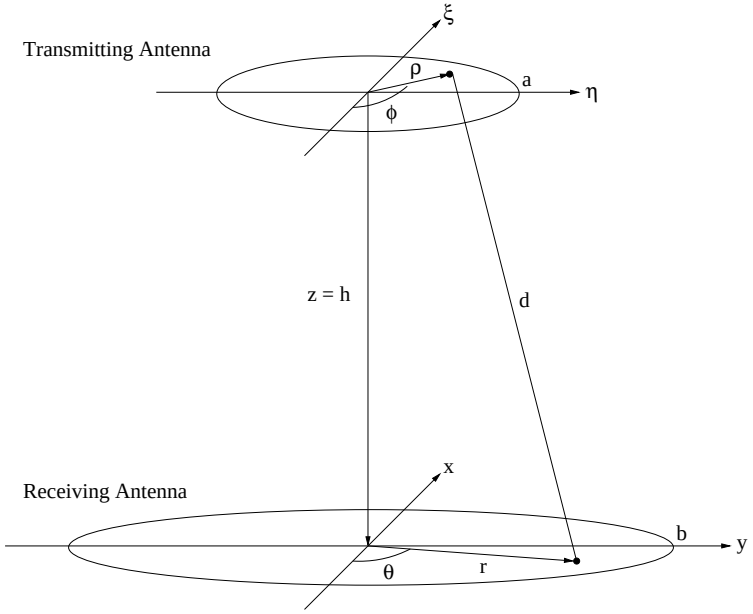

Figure 1: Diffraction geometry of the transmitting and receiving phased-array antennas.

While the Huygens-Frensel principle fully describes the propagation of the electromagnetic radiation transmitted from the phased-array antenna to some plane of observation, in general, it is often useful for analysis purposes to simplify this expression further by introducing additional approximations. The first approximation concerns the distance d appearing in Equation (6). Here, we rewrite the distance d by factoring the distance between the planes, z, outside the expression for d, yielding

$$d = z\sqrt{1 + \left(\frac{x-\xi}{z}\right)^2 + \left(\frac{y-\eta}{z}\right)^2}. \tag{8}$$

We then apply a binomial expansion to the resulting square root term in this expression such that

$$d = z\left\{1 + \frac{1}{2}\left[\left(\frac{x-\xi}{z}\right)^2 + \left(\frac{y-\eta}{z}\right)^2\right] - \frac{1}{8}\left[\left(\frac{x-\xi}{z}\right)^2 + \left(\frac{y-\eta}{z}\right)^2\right]^2 + \cdots\right\}. \tag{9}$$

Approximating the occurrence of d appearing in the exponential of the Huygens-Fresnel principle by retaining only the first two terms of the binomial expansion and only the first term of the expansion for the d^2 term in the denominator, after some algebra, it can be shown that Equation (6) reduces to

$$U(x,y) = \frac{e^{ikz}e^{ik(x^2+y^2)/2z}}{i\lambda z}\int_{-\infty}^{\infty}\int_{-\infty}^{\infty}\left[U(\xi,\eta)\; e^{ik(\xi^2+\eta^2)/2z}\right]e^{-ik(x\xi+y\eta)/z}\; d\xi\; d\eta. \tag{10}$$

This result is known as the Fresnel approximation and is valid when distance z satisfies the condition [8]

$$z^3 \gg \max\left\{\frac{k}{8}\left[(x-\xi)^2+(y-\eta)^2\right]^2\right\}. \tag{11}$$

In effect, the condition given by Equation (11) limits how close the observation plane may be to plane of the transmitting antenna in terms of the wavelength of the transmitted radiation and limits the relative size of the antenna to the area of the observation region where the Frensel approximation will remain valid in the observation plane.

A more stringent approximation to the the Huygens-Fresnel principle which greatly simplifies the analysis of the transmission of electromagnetic radiation from the phased-array antenna is the so-called Fraunhoffer approximation. According to Equation (10), the observed electromagnetic field distribution, $U(x,y)$, is a Fourier transform of the product of the field distribution across the transmitting antenna, $U(\xi,\eta)$, and a quadratic phase factor, $\exp\left[ik(\xi^2+\eta^2)/2z\right]$. If in addition to the condition given by Equation (11) the stronger condition

$$z \gg \max\left[\frac{k}{2}\left(\xi^2+\eta^2\right)\right] \tag{12}$$

is satisfied [8], then the quadratic phase factor under the integrals of the Fresnel approximation is approximately one over the entire surface area of the transmitting antenna and Equation (10) reduces to

$$U(x,y) = \frac{e^{ikz}e^{ik(x^2+y^2)/2z}}{i\lambda z}\int_{-\infty}^{\infty}\int_{-\infty}^{\infty} U(\xi,\eta)\; e^{-ik(x\xi+y\eta)/z}\; d\xi\; d\eta. \tag{13}$$

Therefore, under the Fraunhoffer approximation, the observed field can be found directly from a Fourier transform of the transmitted field distribution itself.

Since the phased-array antenna transmitting the electromagnetic radiation is assumed to be circular, it is natural to exploit this circular symmetry by transforming the Fraunhoffer approximation to polar coordinates. The transformation from Cartesian coordinates to polar coordinates in the plane of the antenna and the plane of observation are given by the following relations:

$$\begin{aligned} r &= \sqrt{x^2+y^2} & x &= r\cos(\theta) \\ \theta &= \arctan\left(\frac{y}{x}\right) & y &= r\sin(\theta) \\ \rho &= \sqrt{\xi^2+\eta^2} & \xi &= \rho\cos(\phi) \\ \phi &= \arctan\left(\frac{\eta}{\xi}\right) & \eta &= \rho\sin(\phi). \end{aligned} \tag{14}$$

The geometry of this transformation between the Cartesian coordinates considered above and the new polar coodinates is illustrated in Figure 1. Under this transformation of coordinates, the Fraunhoffer approximation (Equation (13)) becomes

$$U(r,\theta) = \frac{e^{ikz\left(1+\frac{r^2}{2z^2}\right)}}{i\lambda z}\int_0^{\infty}\int_0^{2\pi} U(\rho,\phi)\; e^{-ikr\rho\cos(\phi-\theta)/z}\; \rho\; d\rho\; d\phi. \tag{15}$$

To simplify Equation (15) further, we first seperate the radial and angular dependence of the phased-array antenna's field distribution by expanding this function in terms of a Fourier series, namely,

$$U(\rho,\phi) = \sum_{n=-\infty}^{\infty} U_n(\rho)\; e^{in\phi}, \tag{16}$$

where the radial Fourier coefficients are given by

$$U_n(\rho) = \frac{1}{2\pi}\int_0^{2\pi} U(\rho,\phi)\; e^{-in\phi}\; d\phi. \tag{17}$$

Substituting the Fourier series expansion of the field distribution into Equation (15) yields

$$U(r,\theta) = \frac{e^{ikz\left(1+\frac{r^2}{2z^2}\right)}}{i\lambda z} \sum_{n=-\infty}^{\infty} \int_0^{\infty} \int_0^{2\pi} U_n(\rho)\ e^{in\phi - ikr\rho\cos(\phi-\theta)/z}\ \rho\ d\rho\ d\phi. \tag{18}$$

By considering a change of variables for the angular coordiantes in the integral of Equation (18), we can now simplify Equation (18) considerably. If we let

$$\phi - \theta = \beta + \frac{3\pi}{2}, \tag{19}$$

then changing the variable of the angular coordinate in integral of Equation (18) from ϕ to β yields

$$U(r,\theta) = \frac{e^{ikz\left(1+\frac{r^2}{2z^2}\right)}}{i\lambda z} \sum_{n=-\infty}^{\infty} e^{in\left(\theta+\frac{3\pi}{2}\right)} \int_0^{\infty} \int_{-\theta-\frac{3\pi}{2}}^{2\pi-\theta-\frac{3\pi}{2}} U_n(\rho)\ e^{i\left[n\beta - \frac{kr\rho}{z}\sin(\beta)\right]}\ \rho\ d\rho\ d\beta. \tag{20}$$

The integral in Equation (20) over the new angular coordinate β is now simply given by the Bessel function identity

$$J_n(x) = \frac{1}{2\pi} \int_{\alpha}^{2\pi+\alpha} e^{i[n\beta - x\sin(\beta)]}\ d\beta, \tag{21}$$

where $J_n(x)$ is the nth-order Bessel function. Writing Equation (20) in terms of Bessel functions, we find that

$$U(r,\theta) = \frac{ke^{ikz\left(1+\frac{r^2}{2z^2}\right)}}{iz} \sum_{n=-\infty}^{\infty} (-i)^n e^{in\theta} \int_0^{\infty} U_n(\rho)\ J_n\left(\frac{kr\rho}{z}\right)\ \rho\ d\rho. \tag{22}$$

However, if the electromagnetic field distribution transmitted by the phased-array antenna, $U(\rho,\phi)$, is also circularly-symmetric, that is, if $U(\rho,\phi) = U(\rho)$, then the radial Fourier coefficients in Equation (22) are given by

$$U_n(\rho) = \begin{cases} U(\rho) & \text{for } n = 0 \text{ and} \\ 0 & \text{for all } n \neq 0. \end{cases} \tag{23}$$

Therefore, when the phased-array antenna and its transmitted field distribution are circularly-symmetric, the electromagnetic field in the observation plane is simply given by a Hankel transform of the form

$$U(r) = \frac{ke^{ikz\left(1+\frac{r^2}{2z^2}\right)}}{iz} \int_0^{\infty} U(\rho)\ J_0\left(\frac{kr\rho}{z}\right)\ \rho\ d\rho, \tag{24}$$

where J_0 is the zeroth-order Bessel function.

Non-Dimensionalization

In the following sections, we outline the spectral and pseudo-spectral optimization techniques that are used to solve the power beaming problem considered in this report. However, in order to simplify the discussion on the development and implementation of these techniques, we begin here by first rewriting the Fraunhoffer approximation for the transmitting phased-array antenna derived in the previous section in a non-dimensionalized form. This non-dimensionalized form of the Fraunhoffer approximation will then be used throughout the remainder of this report.

Because the complex scalar component of the transmitted electromagnetic field distribution, $U(\rho)$, is only non-zero on the surface of the transmitting phased-array antenna, which is assumed here to be a circle of radius a, Equation (24) can be written more precisely as

$$U(r) = \frac{ke^{ikz\left(1+\frac{r^2}{2z^2}\right)}}{iz} \int_0^{a} U(\rho)\ J_0\left(\frac{kr\rho}{z}\right)\ \rho\ d\rho. \tag{25}$$

In order to non-dimensionalize Equation (25), we first rescale the radial coordinate in the plane of the transmitting antenna, ρ, by the radius of the transmitting antenna itself. Denoting the new radial coordinate with a prime symbol, this rescaling yields

$$\rho' = \frac{\rho}{a}. \tag{26}$$

Under this change of radial coordinates, Equation (25) becomes

$$U(r) = \frac{ka^2 e^{ikz\left(1+\frac{r^2}{2z^2}\right)}}{iz} \int_0^1 U(\rho')\ J_0\left(\frac{ka}{z} r\rho'\right)\ \rho'\ d\rho'. \tag{27}$$

In addition, we also rescale the wavenumber of the transmitted electromagnetic radiation, k, and the distance between the two antennas, z, by the radius of the transmitting antenna such that

$$k' = ka \qquad \text{and} \qquad z' = \frac{z}{a}. \tag{28}$$

It then follows that

$$U(r) = \frac{k'}{iz'} \exp\left\{ik'z'\left[1 + \frac{1}{2}\left(\frac{r}{az'}\right)^2\right]\right\} \int_0^1 U(\rho')\ J_0\left(\frac{k'}{az'} r\rho'\right)\ \rho'\ d\rho'. \tag{29}$$

Next, we rescale the radial coordinate in the plane of the receiving antenna, r, in terms of the rescaled wavenumber, k', the rescaled distance, z', and the radius of the transmitting antenna, a. The new radial coordinate in the plane of the receiving antenna is defined as

$$r' = \frac{k'}{az'} r. \tag{30}$$

Inserting r' into Equation (29) yields

$$U(r') = \frac{k'}{iz'} \exp\left\{ik'z'\left[1 + \frac{1}{2}\left(\frac{r'}{k'}\right)^2\right]\right\} \int_0^1 U(\rho')\ J_0\left(r'\rho'\right)\ \rho'\ d\rho'. \tag{31}$$

Finally, if we subsume the phase term outside the integral in Equation (31) into the left-hand-side of the equation, combining it with the received field distribution, $U(r')$, then we can rewrite Equation (31) as

$$H(r') = \int_0^1 U(\rho')\ J_0\left(r'\rho'\right)\ \rho'\ d\rho', \tag{32}$$

where

$$H(r') = \frac{iz'}{k'} \exp\left\{-ik'z'\left[1 + \frac{1}{2}\left(\frac{r'}{k'}\right)^2\right]\right\} U(r') \tag{33}$$

is the new, rescaled field distribution in the plane of the receiving antenna.

Equation (32) is the non-dimensionalized form of the Franhoffer approximation used to solve the power beaming problem with the spectral and pseudo-spectral optimization methods described in the following sections. However, note that in the following sections the primed notation used above is dropped and is replaced with the notation $x \equiv \rho'$ and $y \equiv r'$ such that Equation (32) can be written more concisely as

$$H(y) = \int_0^1 U(x)\ J_0(xy)\ x\ dx. \tag{34}$$

Spectral Method

As stated in the introduction of this report, in order to achieve the ideal efficiency in converting the power from the transmitted microwave beam to usable energy, the electromagnetic field intensity on the receiving antenna should be distributed as uniformly as possible across the surface of the receiving antenna and as much of the beam intensity as possible should fall on the receiving antenna. The energy is given by

$$E_{received} = \int_0^b H(y)^2 \; y \; dy, \tag{35}$$

where, by Parseval's Theorem and conservation of energy,

$$E_{total} = \int_0^\infty U(x)^2 \; x \; dx \; = \int_0^\infty H(y)^2 \; y \; dy. \tag{36}$$

The intensity peaks, or side-lobes, that do not fall on the receiving antenna should be as small as possible in order to limit interference with off-site electronics and, more importantly, minimize possible health risks to humans. Note that a distribution function that satisfies these requirements perfectly is the step function which is nonzero only on the receiving antenna. Using the non-dimensionalized variables from the previous section and supposing for the moment a receiver radius of one, the ideal distribution function has the form:

$$H_{ideal}(y) = \begin{cases} \sqrt{2} & 0 \le y \le 1 \\ 0 & y > 1 \end{cases} . \tag{37}$$

The distribution $U(x)$ on the transmitting antenna which will generate the ideal distribution is given by the inverse Hankel transform:

$$U_{ideal}(x) \propto \int_0^\infty H_{ideal}(y) \; J_0(xy) \; y \; dy \; = \int_0^1 J_0(xy) \; y \; dy \; = \frac{J_1(x)}{x}. \tag{38}$$

However, this function is not a compactly supported. Note that any transmitting satellite antennae are limited in size by certain practical constraints. We therefore need a distribution function $U(x)$ which is nonzero only on a finite region, does not vary significantly over small distances, and has a Hankel transform $H(y)$ that satisfying our constraints on the receiving antenna.

Spectral-type methods are well suited to calculate a distribution function on the transmitting antenna, because they allow for analytic transformation between the input function $U(x)$ and the output function $H(y)$. Moreover, once we have found an appropriate $H(y)$, $U(x)$, these can be guaranteed to be compactly supported, i.e., be nonzero only on a finite region.

We can express $U(x)$ as a weighted sum of basis functions $u_p(x)$ such that for some constants a_p,

$$U(x) = \sum_{p=0}^{\infty} a_p u_p(x). \tag{39}$$

However, in order to develop a numerical optimization method with finite function evaluations, we must truncate this sum at some $P > 0$, resulting in a finite linear combination, $U(x) = \sum_{p=0}^{P} a_p u_p(x)$. We assume that $U(x) = 0$ for $x > 1$ to make the input field physically realizable, we then have (up to a constant multiple):

$$H(y) = \int_0^1 U(x) J_0(xy) x dx = \sum_{p=0}^{P} a_p \int_0^1 u_p(x) J_0(xy) x dx. \tag{40}$$

To facilitate the compact support constraint, let $h_p(y) = \int_0^1 u_p(x) J_0(xy) x dx$, and hence, we can write H as,

$$H(y) = \sum_{p=0}^{P} a_p h_p(y). \tag{41}$$

Now by choosing u_p wisely, such that the integral for h_p can be performed analytically, we then can find an ideal $H(y)$ such that $U(x) = 0$ for all $x > 1$; thus producing the desired $H(y)$ when Hankel transformed.

We have a number of options from which to choose our basis functions u_p. We chose a basis that has been used previously for this problem, the set of so-called tapered beam functions, $u_p(x) = (1 - x^2)^{p-1}$ on $0 \leq x \leq 1$ [9]. These beam functions are mapped into $h_p \propto \frac{J_p(x)}{x^p}$ via the Hankel transform. Although this only gives us terms of even order in x, by the Stone-Weierstrass approximation theorem on a compact interval, any continuous function can be approximated uniformly by a polynomial. For example, the Bernstein polynomials, which are given by

$$B_n(z) = \sum_{k=0}^{n} \binom{n}{k} z^k (1-z)^{n-k} U(\frac{k}{n}), \tag{42}$$

converge uniformly to a function U on $[0, 1]$. Therefore, by setting $z = x^2$, we see that there exists a sequence of polynomials in x^2 that converge uniformly to any continuous function U on $[0, 1]$ [10]. Furthermore, when using a series expansion with the tapered beam basis functions converge uniformly to the optimal function U as long as it is continuous. Unfortunately, however, this does not give us any information about the rate of convergence.

Having posed the spectral method to solve the power beaming problem above, we can now implement a numerical code to find the set of coefficients a_p for our basis functions h_p which produce the optimal distribution $H(y)$. Once these coefficients have been found for the optimal receiver distribution, we will simultaneously have found the compactly supported transmitter distribution needed to produce the corresponding receiver distribution.

The spectral method was implemented numerically using MATLAB's FMINCON routine, which finds a constrained minimum of a function of several variables. The objective function constructed here aims to balance the competing requirements that the intensity of the received field distribution be as uniformly distributed across the surface of the receiving antenna as possible, while simultaneously maximizing the energy transmission efficiency between the two antennas. The objective function has the following form:

$$\min_{a_1, a_2, \ldots, a_P} \left[W_1 \, ||H'(y)|| + W_2 \frac{\int_0^b H(y)^2 \; y \; dy}{\int_0^1 U(x)^2 \; x \; dx} \right], \tag{43}$$

where the weights W_1 and W_2 may be chosen by the user to emphasize one of the two requirements. Note that the energy integrals, as well as $H'(y)$, can be evaluated analytically for the chosen basis functions, which makes the spectral method attractive both from an implementation and analytic perspective.

The results obtained with the spectral implementation when $W_2 >> W_1$ are shown in Figures 2 and 3. For this case, the optimization routine attempts to make the energy as large as possible while ignoring the flatness constraint. The resulting beam field profiles are normalized and plotted within the transmitter's region from [0,1]. As illustrated in Figure 2, the normalized profiles are similar. However, increasing the radius flattens the profile as it reaches the transmitter's boundary. The normalized receiving field is shown in Figure 3. As expected, the energy captured increases with the radius. The increase in radius also has the beneficial effect of diminishing the side-lobes.

In some applications the receiver must have a nearly constant field, and hence, the associated W_1 term becomes important. In this case, both the transmitter's and receiver's profile change significantly, as can be seen in Figures 4 and 5. The flatness constraint becomes more pronounced as the radius increases, which increase the side-lobes (see Figure 5). With the increase in side-lobes, the energy received drops significantly with increasing radius. For instance, the energy received drops by approximately 0.02% when the radius is one, but when the radius is four, the drop is closer to 30%.

The numerical code developed here for the spectral method can be easily modified to incorporate intensity limitations due to human health concerns or limits due to electromagnetic equipment near the receiving antenna. In addition, the method is flexible enough to incorporate realistic estimates of the receiver's efficiency for different distributions. In the following section, we find the optimal transmitted field via a pseudo-spectral method, trading the analytic simplicity of the spectral approach to increase the method's generality.

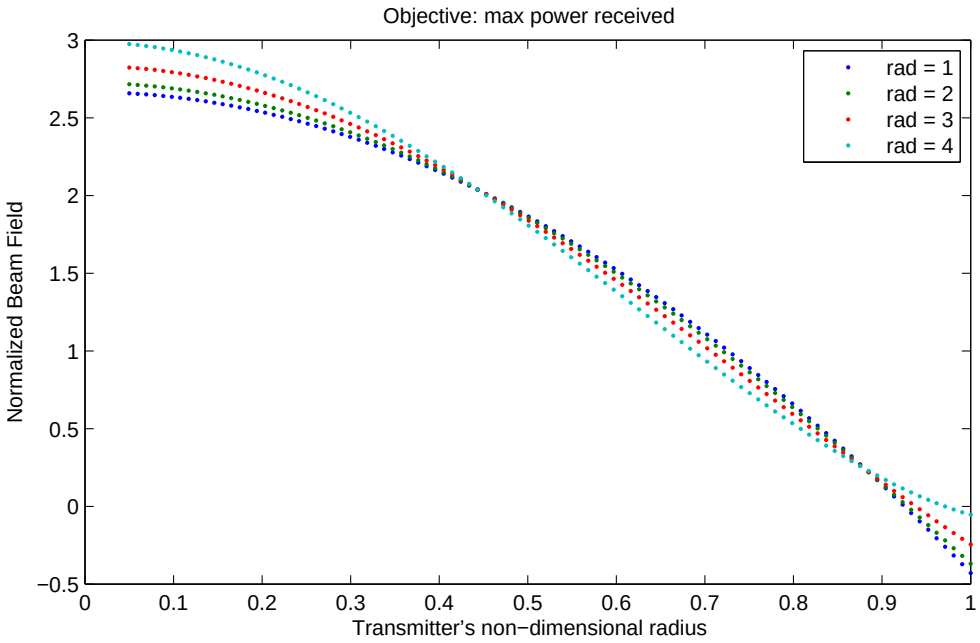

Figure 2:

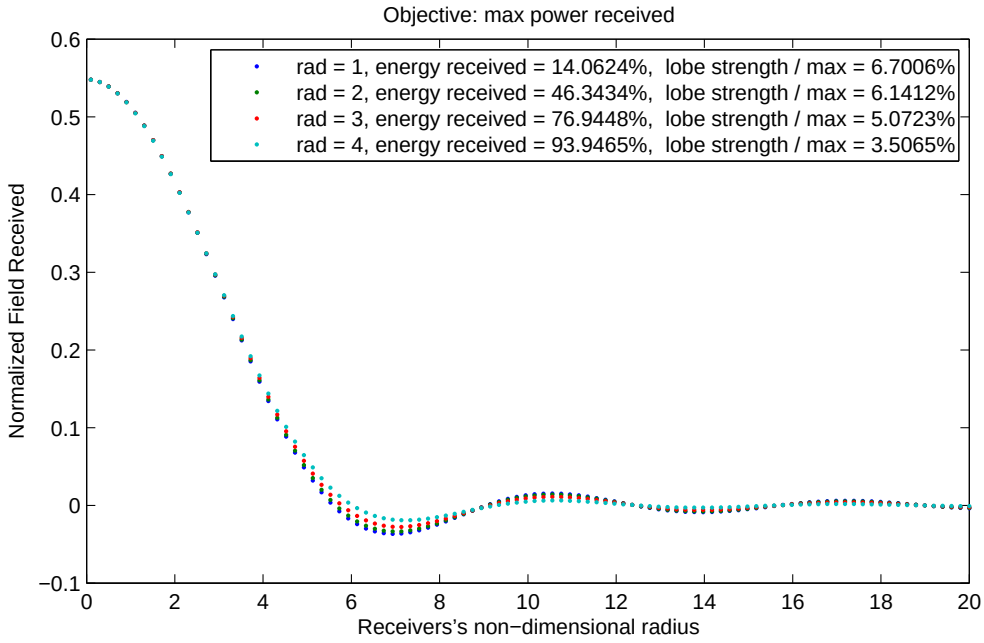

Figure 3:

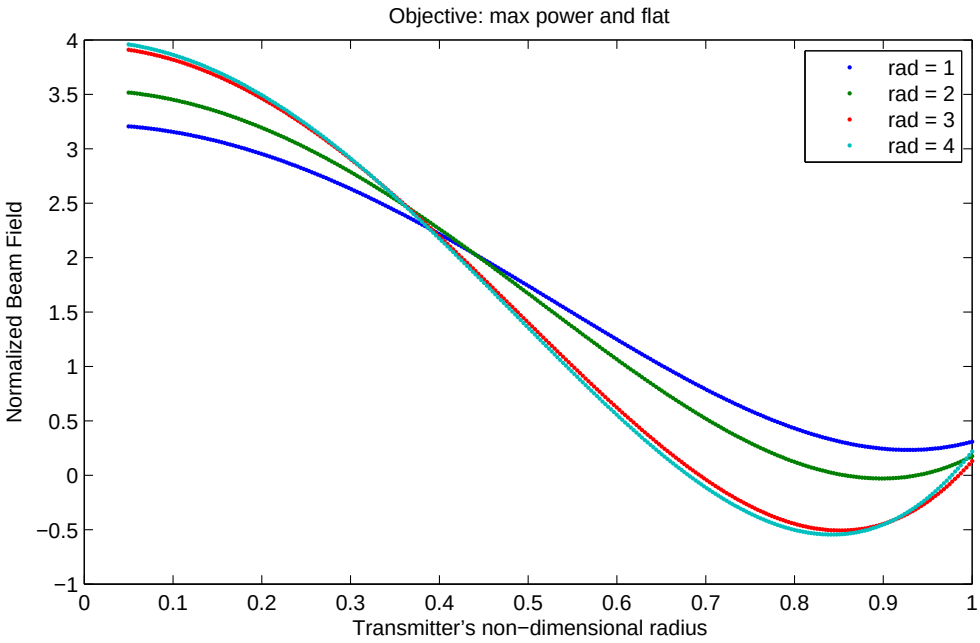

Figure 4:

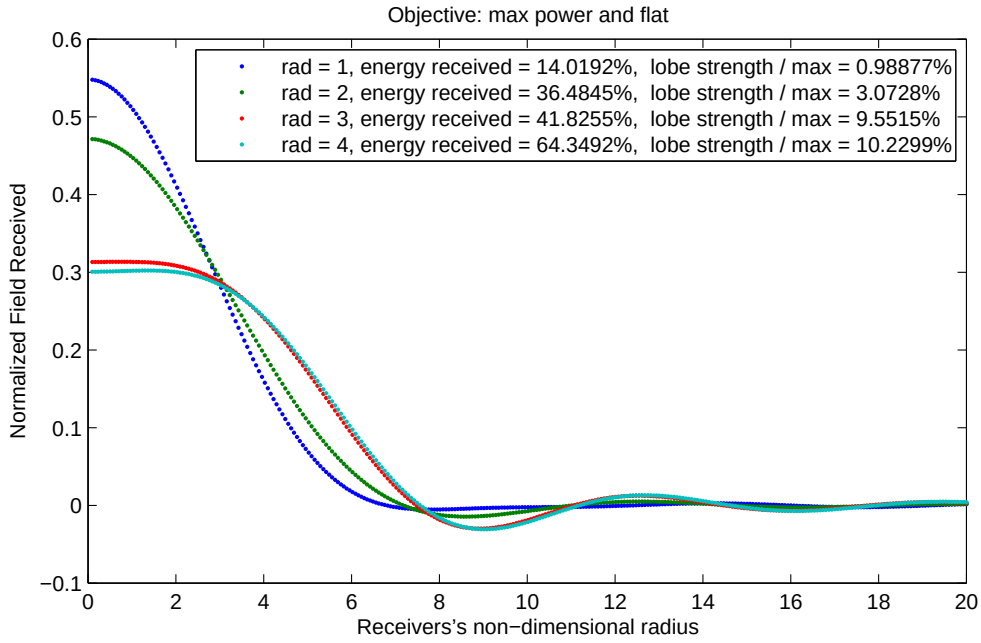

Figure 5:

Pseudo-Spectral Method

We now treat the problem outlined in the previous section as a control system. A control system model can be defined as an input-to-output mathematical transformation. To achieve desired performance, control profiles are often designed so that a performance function is minimized or maximized. Analytic optimal control designs are based on solutions of the Hamilton-Jacobi-Bellman's equation and/or Pontryagin's minimum principle. However, analytic solutions for even moderately complex systems are extremely difficult to find, if not impossible. On the other hand, numerical approximate optimal controls can be computed using the pseudo-spectral optimal control method (PS optimal control), which has been applied to many engineering problems from the attitude control of the International Space Station [11] to satellite formation design [12]. The method is based on the pseudo-spectral approximation. Given an input or output function, $f(t) : [a, b] \rightarrow \Re$, the function is approximated at Legendre-Gauss-Lobatto (LGL) quadrature nodes, $f(t_0), f(t_1), \cdots, f(t_N)$ (collocation from other orthogonal polynomials can also be used, such as Chebyshev-Gauss-Lobatto nodes). The LGL nodes, $t_0 = -1 < t_1 < \cdots < t_N = 1$, are defined by

$$\begin{array}{l} t_0 = -1, \;\; t_N = 1, \text{ and} \\ \text{for } k = 1, 2, \ldots, N-1, t_k \text{ are the roots of } \dot{L}_N(t) \end{array}$$

where $\dot{L}_N(t)$ is the derivative of the N-th order Legendre polynomial $L_N(t)$. It is a known result in approximation theory that the polynomials of interpolation using the value of $f(t)$ at the LGL nodes converge to $f(t)$ under the L^2 norm at the rate of $1/N^m$, where m is the smoothness of $f(t)$. If $f(t)$ is C^∞, then the polynomial interpolation at the LGL nodes converges at a spectral rate, i.e. it is faster than any given polynomial rate.

A problem of optimal control is defined using differential and integral transformations. In the corresponding discrete problem, differentiation is approximated by the following matrix multiplication

$$\left[\begin{array}{cccc} \dot{f}^N(t_0) & \dot{f}^N(t_1) & \cdots & \dot{f}^N(t_N) \end{array} \right]^T = D(\bar{x}_i^N)^T \tag{44}$$

where $f^N(t)$ is the interpolating polynomial of $f(t_0), \cdots, f(t_N)$, D is the $(N+1) \times (N+1)$ differentiation matrix defined by

$$D_{ik} \;\; = \;\; \left\{ \begin{array}{ll} \frac{L_N(t_i)}{L_N(t_k)} \frac{1}{t_i - t_k}, & \text{if } \; i \neq k; \\ -\frac{N(N+1)}{4}, & \text{if } \; i = k = 0; \\ \frac{N(N+1)}{4}, & \text{if } \; i = k = N; \\ 0, & \text{otherwise} \end{array} \right.$$

An integration is approximated by the Gauss-Lobatto integration rule,

$$\int_{-1}^{1} f(t) dt \;\; = \;\; \sum_{k=0}^{N} f(t_k) w_k$$

where w_k are the LGL weights defined by

$$w_k \;\; = \;\; \frac{2}{N(N+1)} \frac{1}{[L_N(t_k)]^2},$$

The approximating integral has zero error if $f(t)$ is a polynomial of degree less than or equal to $2N - 1$, which almost doubles of the number of nodes [13].

Now consider the non-dimensionalized version of the problem of power beaming. The signal or field at the transmitter is denoted by $U(x)$, which is considered as the control input of the system. The output is the field at the receiver, denoted by $H(y)$. The input-output relationship is defined by Hankel transformations

$$
\begin{aligned}
&H(y) = \int_0^\infty U(x) J_0(xy) x dx \\
&U(x) = \int_0^\infty H(y) J_0(yx) y dy \\
&\text{Subject to} \\
&U(x) = 0, \text{ if } x > 1 \\
&\int_0^1 U^2(x) x dx = 1 \\
&H_{min}(y) \leq H(y) \leq H_{max}(y) \\
&U_{min}(x) \leq U(x) \leq U_{max}(x)
\end{aligned}
$$

The upper and lower bounds of both $U(x)$ and $H(y)$ can be either a constant or a function. An illustrative diagram of the system is shown in Figure 6.

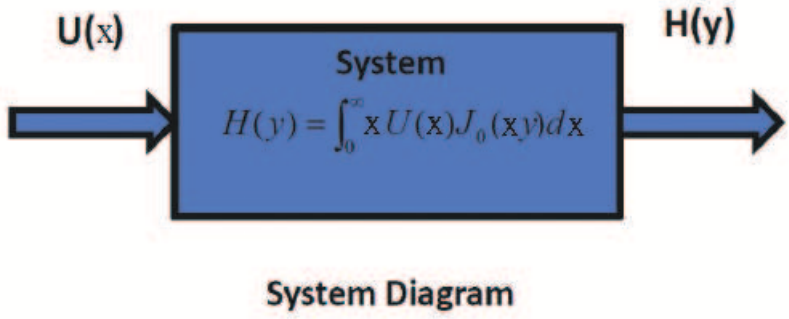

Figure 6: An illustrative diagram of the system.

For the performance, the goal is to balance between the desired shape of $H(y)$ and the total energy at the receiver. If a desired $H(y)$ is a constant, a cost function can be designed as follows

$$J(U(\cdot), W_1, W_2) = W_1 V(H(\cdot))_0^b + W_2 \int_0^b y H(y)^2 dy$$

where $V(H(\cdot))_0^b$ is a measure of variation of $H(y)$ in the interval $[0, b]$. For constant valued functions, $V(H(\cdot)) = 0$. In this functional, W_1 and W_2 are weights selected based on the requirements from users. A larger value of W_2 implies that the main goal is to receive more energy, while achieving a flat shape for $H(y)$ is a secondary consideration. On the other hand, a large W_1 implies that the first priority is to shape the function $H(y)$ and a small energy transfer ratio is acceptable.

If for any given target state $H_{target}(y)$, there always exists a control under which the system achieves the target state, then the system is called reachable. Because the Hankel transform is invertible, the system with $x \in [0, \infty)$ is reachable. However, the problem addressed in this report is not reachable because of the constraint $U(x) = 0$ for $x > 1$. This is a fundamental reason why a flat $H(y)$ cannot be achieved completely, as shown by the simulations. This property of unreachability will have its impact on other cases of power beaming. For a desired target profile of $H(y)$, it is likely that there is no $U(x)$ that can achieve this target. The best we can do is to set up a cost function to make $H(y)$ as close as possible, i.e. optimization.

If the desired shape for $H(y)$ is not flat, then the cost function has to be modified. Instead of $V(H(\cdot))_0^b$, a functional $F(U(\cdot), \lambda)$ must be designed to reflect the shape requirement. Such a functional can be a linear combination of differential and integral operators with some known or unknown parameters. In the case that λ is unknown, it must be treated as an additional optimization variable. Using the differentiation matrix and Gauss-Lobatto integration rule introduced above, the PS optimal control method is able to accommodate various types of cost functions. For the purpose of illustration, we use $V(H(\cdot))_0^b$ as the cost in this report.

For the purpose of numerical computation, the entire problem is approximated at a set of LGL nodes. For example, the input function $U(x)$ is approximated by a vector

$$\begin{bmatrix} \bar{U}_0 & \bar{U}_1 & \cdots & \bar{U}_N \end{bmatrix}^T$$

where $\bar{U}_i = U(x_i)$ and $x_0 = 0 \leq x_1 \leq \cdots \leq x_N = 1$ are the LGL nodes. The original problem of optimal control is transformed into the following finite dimensional optimization problem.

$$\begin{aligned}
&\min_{(\bar{U}_0,\bar{U}_1,\cdots,\bar{U}_N)} \left(\sum_{i=1}^{N^y-1} (\bar{H}_{i+1} - \bar{H}_i)^2 + \sum_{i=0}^{N^y} x_i \bar{H}_i^2 w_i^y \right) \\
&\text{Subject to} \\
&H_j = \sum_{i=0}^{N^x} \bar{U}_i J_0(x_i y_j) x_i w_i^x, \qquad j = 0, 1, \cdots, N^y \\
&\sum_{i=0}^{N^x} x_i \bar{U}_i^2 = 1 \\
&H_{\min} \leq \bar{H}_i \leq H_{max}, \qquad i = 1, 2, \cdots, N^y \\
&U_{min} \leq \bar{U}_i \leq U_{max}, \qquad i = 1, 2, \cdots, N^x
\end{aligned} \tag{45}$$

The problem defined by (45) is a constrained optimization problem in $\Re^{N^x}$. It can be solved by using sequential quadratic programming. This approach is implemented in MATLAB and simulations are carried out.

To test the algorithm, a sequence of simulations were carried out. The results of these simulations are summarized in Figure 7. Here, we apply some constraints to the simulations, namely,

$$U_{min} = 0 \quad \text{and} \quad H_{max} = 1. \tag{46}$$

We use a constant weight $W_2 = 1$ for the energy part of the cost function. For W_1, three different cases are studied: $W_1 = 1$, $W_1 = 100$, and $W_1 = 10000$. Note that as the weight is increased H(y) becomes increasingly flat. The results are plotted in blue, red, and green, respectively. The stars in Figure 7 represent the discrete solution by solving (45). When $W_2 = 1$, about 95.43% of energy is received by the receiver. However, the curve is not as flat. If $W_2 = 100$, about 43.97% of energy is received. If $W_2 = 10000$, the curve is really flat, but only about 5.28% of the energy is received.

To check the behavior of $H(y)$ beyond the radius of the antenna, the value of $H(y)$ is computed using quadrature integration in MATLAB. The result is shown in Figure 8. The behavior of $H(y)$ is normal without undesired peaks.

To summarize, the method of PS optimal is applied to the problem. This formulation has the flexibility of accommodating various constraints, for instance upper and lower bounds for both $U(x)$ and $H(y)$. The framework allows one to combine multiple tasks, such as fitting a target curve and maximizing the energy received, in a single problem formulation of optimization with weights. Simulations for the case of a flat $H(y)$ using various weights on a laptop PC show that the method converges at a good rate using twenty LGL nodes.

Conclusion and Future Work

In this report, we have considered several optimization techniques useful in the analysis of a power beaming problem of a space-based solar power satellite. We derived, via scalar diffraction theory, the non-dimensional model for power transmission from a space-based satellite to Earth, and found the optimal power profiles under various constraints via spectral and pseudo spectral methods. For the spectral method, we noted its ability to take advantage of analytic results to simplify its numerical implementation, and more importantly, to guarantee a compactly supposed profile from the transmitting antenna. The pseudo-spectral, via a control

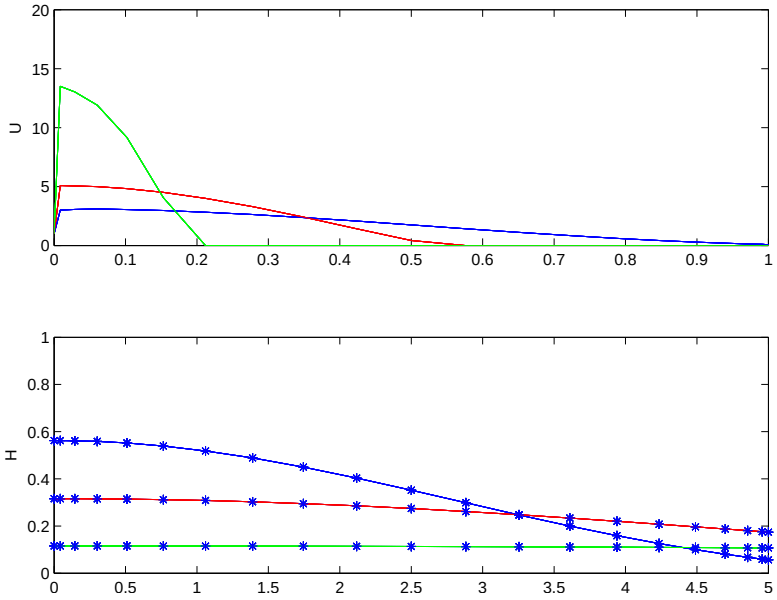

Figure 7: Blue: $W_1 = 1$; red: $W_1 = 100$; green: $W_1 = 1000$; Star: discrete approximation.

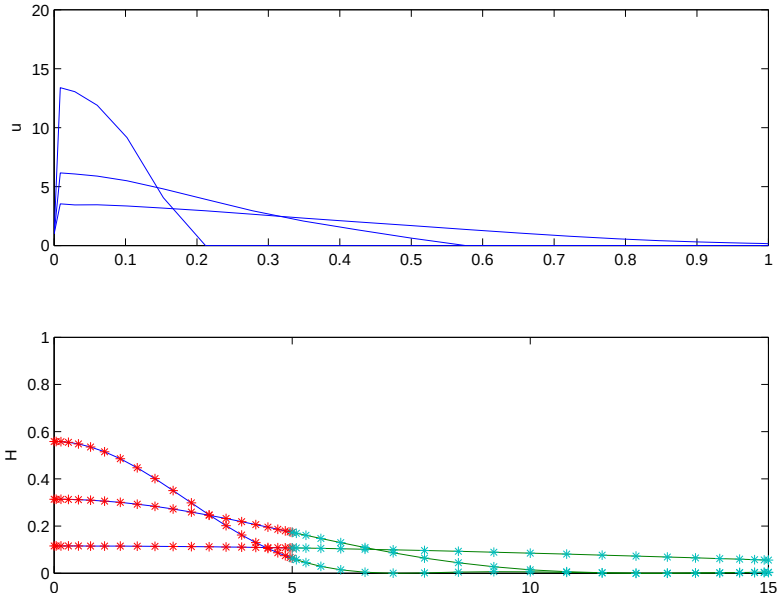

Figure 8: System behavior in an extended range.

theory perspective, was introduced and used to solve our model problem. While both approaches have their strengths, the pseudo-spectral method is better suited for more general problems and will be investigated further.

There are several interesting research avenues which remain open to further investigation that are of interest. We did not pursue any convergence results on the spectral method, which are of interest for use of this method as a physical preconditioner for more general problems. In the case of more general models, it would be interesting is to consider multiple sources, from different satellites orbiting the Earth with their own dynamics. Another interesting extension is to consider multiple receiving stations, where the transmitted beam would be tapered in such a way as to maximize the incoming energy at each receiving antenna, while simultaneously having a compactly supported profile at the transmitting antenna.

Acknowledgements

First and foremost, we would like to thank Seth Potter of The Boeing Company for presenting this problem to us at the Claremont Colleges Math-in-Industry Workshop 2009. His comments and suggestions on the formulation of the problem were invaluable in the work presented here. In addition, we would also like to thank the Claremont Center for Mathematical Sciences, EcoArray, the Center for Quantitative Life Sciences at Harvey Mudd College, the Institute for Pure and Applied Mathematics at UCLA, ISI, the National Science Foundation, and the Oxford Cener for Collaborative Applied Mathematics for their sponsorship of the Claremont Colleges Math-in-Industry Workshop 2009.

References

[1] N. S. Lewis and D. G. Nocera, *Proc. Natl. Acad. Sci. USA*, **103**, 15792 (2006).

[2] N. S. Lewis, *MRS Bulletin*, **32**, 808 (2007).

[3] D. Craddock, *Renewable Energy Made Easy: Free Energy from Solar, Wind, Hydropower, and Other Alternative Energy Resources*, Atlantic Publishing Group, Inc., 2008.

[4] P. E. Glaser, *Science*, **162**, 857 (1968).

[5] P. E. Glaser, *Proc. IEEE.*, **65**, 1162 (1977).

[6] P. E. Glaser, *IEEE. Trans. Microwave Theory Tech.*, **40**, 1230 (1992).

[7] P. E. Glaser, *Phys. Today*, **30**, 30 (1977).

[8] J. W. Goodman, *Introduction to Fourier Optics*, The McGraw-Hill Companies, Inc., 1996, 2nd edn.

[9] S. D. Potter, *Space Power*, **13**, 185 (1994).

[10] N. J. Pippenger, Private communications (2009).

[11] W. Kang and N. Bedrossian, *SIAM News*, **September** (2007).

[12] I. M. Ross and W. Kang, *NPS-AFRL Report*, **December** (2007).

[13] C. Canuto, M. Y. Hussaini, A. Quarteroni, and T. A. Zang, *Spectral Method in Fluid Dynamics*, Springer-Verlag, 1988.